THE ASTROPHYSICAL JOURNAL, 434:L25–L28, 1994 October 10

THE PSR 1800−21/G8.7−0.1 ASSOCIATION: A VIEW FROM *ROSAT*

JOHN P. FINLEY
Department of Physics, Purdue University, 1396 Physics Building, West Lafayette, IN 47907-1396;
finley@purds1.physics.prudue.edu

AND

HAKKI ÖGELMAN
Department of Physics, University of Winsconsin-Madison, 1150 University Avenue, Madison, WI 53706;
ogelman@astrog.physics.wisc.edu

Received 1994 May 4; accepted 1994 July 26

ABSTRACT

We present the first imaging X-ray observation of the W30 complex which contains the Galactic SNR G8.7−0.1 and the young radio pulsar PSR 1800−21 as well as a number of discrete ultracompact H II regions. The pulsar PSR 1800−21 is detected as a count rate of 1.5 ± 0.5 ks^{-1} and diffuse emission from the northern extent of G8.7−0.1 is observed. The data support an association of G8.7−0.1 and PSR 1800−21, and the peculiar morphology can be explained if the supernova which gave birth to PSR 1800−21 occurred within, or very near, a molecular cloud. The suggested scenario removes the requirement of a large transverse velocity for the pulsar, one of the greatest difficulties with the association.

Subject headings: pulsars: individual (PSR 1800−21) — stars: neutron — supernova remnants — X-rays: stars

1. INTRODUCTION

The W30 complex appears as a large circular region (diameter $\sim 1°$) of radio continuum emission with a number of superposed smaller discrete emission regions (Altenhoff et al. 1978; Reich et al. 1984; Handa et al. 1988). Radio recombination line observations have been used to identify the discrete sources as H II regions and CO observations also show molecular gas associated with W30 (Blitz, Fich, & Stark 1982). The extended component is identified as a Galactic supernova remnant (SNR), G8.7−0.1, on the basis of observed nonthermal emission at 57.5 MHz (Odegard 1986).

Using the VLA at 20 cm and 90 cm wavelengths, Kassim & Weiler (1990a) originally found G8.7−0.1 to be a shell-type remnant. By associating G8.7−0.1 with coincident H II regions with known distances, Kassim & Weiler estimate a distance to the SNR of 6 ± 1 kpc which, combined with its angular size of $\sim 50'$, implies a physical size of ~ 80 pc.

At the southwestern edge of G8.7−0.1 lies the young pulsar ($\tau \sim 17{,}000$ years) PSR 1800−21. The distance to PSR 1800−21 implied by the observed dispersion measure is ~ 5.3 kpc (Clifton & Lyne 1986). The coincidences on the sky, in space, and in age of G8.7−0.1 and PSR 1800−21 have led to a suggested association of the two (Odegard 1986; Kassim & Weiler 1990b). Given the sparsity of SNR/pulsar associations observed in the Galaxy, the possibility of a G8.7−0.1/PSR 1800−21 is intriguing but dynamically problematic. If the pulsar was born at the symmetry center of G8.7−0.1, then to have reached its current position in $\sim 15{,}000$ years requires a transverse velocity of ~ 1700 km s^{-1}. Some possible solutions to the requirement of such a large transverse velocity for the pulsar have been suggested (Kassim & Weiler 1990b) including a reduced distance, increased age, or larger extent of G8.7−0.1 than is presently known.

Very recently a deep new mapping of the W30 region was carried out in the continuum at 327 MHz with spatial resolution comparable to *ROSAT* (Frail, Kassim, & Weiler 1994b). The SNR G8.7−0.1 was found to be more extended than previously thought with a very irregular morphology. Frail et al. (1994b) suggest that the association between SNR G8.7−0.1 and PSR 1800−21 is in jeopardy since no signature (i.e., no pulsar wind nebula) of the high transverse velocity of the pulsar is detected and a more recent estimate of the pulsar's distance based on an improved model of the Galactic electron density (Taylor & Cordes 1993) puts it at ~ 4 kpc, some 1–2 kpc in front of SNR G8.7−0.1.

In this *Letter* we will report on a *ROSAT* observation of the W30 field. The observations will be described in § 2 and the results presented in § 3. A discussion of the implications for the SNR/PSR association can be found in § 4.

2. OBSERVATIONS

The W30 field was observed with the Position Sensitive Proportional Counter (PSPC) at the focus of the X-ray telescope aboard *ROSAT*. Detailed descriptions of the satellite, X-ray mirrors, and detectors can be found in Pfeffermann et al. (1986). The PSPC is sensitive in the soft X-ray energy band 0.1–2.4 keV with an energy resolution of $E/\Delta E \sim 2.3$ at 0.93 keV and an effective spatial resolution of $\sim 25''$ at the center of the focal plane. The data processing was performed with the MIDAS/EXSAS and XSPEC v8.33 packages.

The observations we report on here were acquired in two separate observing sessions; 1992 October 5–1992 October 7 and 1993 March 23. The total exposure time was 11,239 s. The target of the observations was PSR 1800−21, which was in the center of the 2° field of view. PSR 1800−21 was detected at a count rate of 1.5 ± 0.5 ks^{-1} in the 0.1–2.4 keV band. The source position (J2000) was determined to be $\alpha = 18^h3^m50^s.97$ and $\delta = -21°37'8''.5$. This is in excellent agreement with the radio source position (J2000) of $\alpha = 18^h3^m51^s.35$ and $\delta = -21°37'7''.2$ (Taylor, Manchester, & Lyne 1993) given the 6″ uncertainty of the attitude determination. The source detection algorithm was also applied in a medium (M) band (pulse height channels 52–90 corresponding to ~ 0.52–0.90 keV) and a hard ($I + J$) band (pulse height channels 91–201 corresponding to

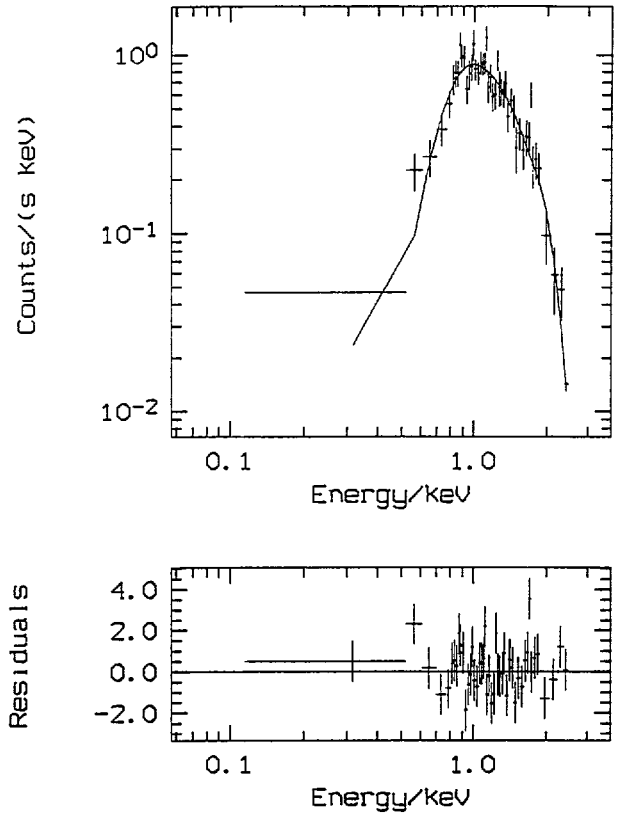

FIG. 2.—Background-subtracted, vignetting, deadtime, and particle background corrected spectrum of G8.7−0.1 in the 0.1–2.4 keV band (*top*) for the region between $l_{II} = 8.^{\circ}6$ and $9.^{\circ}1$ and $b_{II} = 0.^{\circ}5$ and $-0.^{\circ}5$ (see Fig. 1). The smooth curve is the predicted spectrum for a Raymond-Smith thermal plasma with $T_X = 6.6 \times 10^6$ K, solar abundances and an equivalent neutral hydrogen column density of 1.3×10^{22} cm^{-2}. The residuals of the model (in units of σ) are displayed in the bottom panel.

~0.90–2.00 keV). PSR 1800−21 was below the detection threshold in the *M* band, while in the $I + J$ band it was detected at a counting rate of 0.8 ± 0.3 ks^{-1} implying a hard and absorbed spectrum.

The SNR G8.7−0.1 was also detected in this observation. The SNR filled a large portion of the field of view and included the "plume" features described by Frail et al. (1994). The X-ray emission from G8.7−0.1 is prominent in the northern region of the remnant [between Galactic longitudes (l_{II}) $8.^{\circ}6$ and $9.^{\circ}1$ and Galactic latitudes (b_{II}) $-0.^{\circ}5$ and $0.^{\circ}5$]. Emission from elsewhere within the remnant is not detected above the background with any statistical significance. The background-subtracted count rate of the bright northern extent is 0.65 ± 0.05 s^{-1} but the ribs of the PSPC were obscuring some of the emission so this should be treated as a lower limit to the count rate. The background against which this measurement was made was determined by averaging three separate regions at the same off-axis angle as the SNR and is described in more detail in § 3 below.

TABLE 1

PHYSICAL PARAMETERS OF G8.7−0.1

PARAMETER	INITIAL ASSUMPTION	
	$d = 6$ kpc	$E_0 = 10^{51}$ ergs
T_S (10^6 K)	4–8	4–8
V_S (10^2 km s^{-1})	5.3–7.5	5.3–7.5
E_0 (10^{51} ergs)	2–4	1
d (kpc)	6	3.2–4.3
t (10^4 yr)	2.7–3.9	1.5–2.8
n_0 (cm^{-3})	0.02–0.03	0.02–0.04
M_S ($M_\odot$)	365–635	80–160

3. RESULTS

In order to study the spectrum of the diffuse emission associated with G8.7−0.1 the data were "cleaned" (by removal) of contaminating scattered solar X-rays and subsequently corrected for vignetting, dead time, and particle contamination. The X-ray image was, in addition, flat-fielded using energy-dependent exposure maps (Snowden et al. 1994) and smoothed with a 2.′5 (FWHM) Gaussian. A contour plot of the corrected image is displayed in Figure 1*a* (Plate L3) and, for comparison, the radio map of Frail et al. (1994b) is displayed in Figure 1*b* (Plate L4). The position of PSR 1800−21 is marked with a cross in both figures. The pulsar is not apparent in the X-ray image due to the smoothing applied to the data. The effective exposure after corrections was 10,658 s. The data of the bright northern extent were extracted and fitted with a Raymond-Smith thermal plasma model with solar abundances. Due to the large size of the SNR background regions were taken from three independent circles at similar off-axis angles as the diffuse emission region in Figure 1*a* and each was subtracted in turn. The range of the observables found from fitting each of the three background-subtracted spectra separately established our 90% confidence level estimates of neutral hydrogen column density $N_H = (1.2\text{–}1.4) \times 10^{22}$ cm^{-2}, X-ray temperature $T_X = (4\text{–}8) \times 10^6$ K, and an unabsorbed model flux in the 0.1–2.4 keV band of $F_X = (1\text{–}3) \times 10^{-10}$ ergs s^{-1} cm^{-2}. We also derived the electron density $n_e = (0.1\text{–}0.2)\,(6\text{ kpc}/D)^{1/2}$ cm^{-3} from the models normalization constant, K, which is proportional to $(\int n_e^2\, dV)/(4\pi D^2)$. The emitting volume of $V = 10^{60}$ cm^3 was calculated for the extracted region assuming that G8.7−0.1 is a spherical remnant of angular size $\theta_S = 1^{\circ}$ at a distance of 6 kpc. Reduced χ^2 of the spectral fits were ~1 per degree of freedom. Figure 2 displays the spectrum and a representative fit for the set of parameters which yielded the lowest χ^2/DOF. For the adopted distance of 6 kpc to SNR G8.7−0.1 as established by the radio measurements reviewed by Kassim & Weiler (1990a) the corresponding luminosity is (0.4–1.3) $\times 10^{36}$ ergs s^{-1} $(D/6\text{ kpc})^2$. Models in which the element abundances were allowed to vary produced no significant change in the χ^2, and the derived parameters were consistent with those found for the standard Raymond-Smith model with solar abundances.

To search for spectral or absorption variations across the remnant we employed a hardness ratio (HR) defined as the difference in counts between the $I + J$ and *M* bands divided by the sum of counts in the two bands. We calculated HRs for boxes of ~87 arcmin^2 area covering the extent of the radio SNR, 13 in total. No statistically significant variation was observed over the remnant implying that the gradient in the X-ray intensity is not a result of spectral variations or interstellar hydrogen column density variations.

The observed X-ray properties of G8.7−0.1 permit us to derive the physical parameters of the SNR under the assumption that it is a spherically symmetric remnant in the adiabatic phase of evolution. The physical parameters were cast in terms of the observables based upon the work of Hamilton, Sarazin, & Chevalier (1983). The parameters were derived with two different initial assumptions: (1) a distance of 6 kpc, and (2) an

initial energy output of 10^{51} ergs. The results of the calculations for each of the initial assumptions are listed in Table 1, where T_S and V_S are the temperature and velocity of the shock, E_0 is the initial energy, t is the age, n_0 is the ambient density, and M_S is the swept-up mass. We note that recent work (Kassim et al. 1994) on distance determinations to Galactic SNRs based on a Sedov analysis and an initial assumption of $E_0 = 10^{51}$ ergs has been demonstrated on a number of remnants using *ROSAT* data. For the parameters of Table 1 we used a cooling function value of $\Lambda = 3.4 \times 10^{-23}$ ergs cm^3 s^{-1} which was calculated over the bandpass 0.1–2.4 keV using the Raymond & Smith (1977) plasma models. To justify the assumption of a SNR in the adiabatic phase of evolution we also calculated the remnant size expected for the onset of the pressure-driven snowplow phase, $R_{PDS} = 14E_0^{2/7}n_0^{-3/7}\zeta^{-1/7}$ pc, where E_0 is the initial energy in units of 10^{51} ergs, n_0 is the initial ambient density in cm^{-3}, and ζ is a metallicity factor which we take as 1 (solar abundances) (Cioffi, McKee, & Bertschinger 1988). For the two initial assumptions of Table 1 we have $R_{PDS} = 63$ and 93 pc respectively for $d = 6$ kpc and $E_0 = 10^{51}$ ergs, which justify the assumption of an adiabatic phase for G8.7−0.1.

4. DISCUSSION

The PSR 1800−21/G8.7−0.1 association has been considered a weak association (Kassim & Weiler 1990a, b) due to the dynamical problems of the pulsar's position at the edge of the remnant. The recent work of Frail et al. (1994b) only seemed to weaken the case further, since they detect no evidence of a pulsar wind nebula (PWN), which is expected for a pulsar with a high traverse velocity. In addition, the revised distance to PSR 1800−21 of 4 kpc (Taylor & Cordes 1993) places it some 1–2 kpc in front of the SNR, therefore removing the spatial coincidence. Finally, discrepancy between kinematic radial velocities related to G8.7−0.1 and those obtained from H I absorption for PSR 1800−21 (Frail et al. 1991) also indicates a nonassociation of the two. The *ROSAT* data presented here, however, give a new view of the association of PSR 1800−21/G8.7−0.1 which, we will argue, salvages the association and provides a natural explanation for the peculiar morphology which is observed.

4.1. *The Distance to G8.7−0.1*

The parameters of Table 1 for an assumed initial energy, E_0, of 10^{51} ergs yield a distance to G8.7−0.1 of 3.2 kpc $\leq d \leq$ 4.3 kpc. This is in good agreement with the distance to PSR 1800−21 of 3.9 kpc established by Taylor & Cordes (1993) but conflicts with the kinematically determined distance of 6 ± 1 kpc established by Kassim & Weiler (1990a). However, a revision of this distance based upon the recent Galactic rotation model of Brand & Blitz (1993) yields an improved distance estimate of ~4.8 kpc (Frail & Kassim 1994). In addition, an assumed distance of 6 kpc yields an initial energy of $E_0 = (2–4) \times 10^{51}$ ergs, which is somewhat larger than would be expected for a standard supernova explosion. Thus, the data presented here are consistent with G8.7−0.1 and PSR 1800−21 being coincident in space at a distance of ~4 kpc if a standard initial explosion energy of 10^{51} ergs is assumed.

4.2. *The Age of G8.7−0.1*

If G8.7−0.1 is indeed the remnant of the supernova in which PSR 1800−21 was born, the two should have similar ages. The spin-down age of PSR 1800−21 ($\tau = P/2\dot{P}$) is $\sim 1.6 \times 10^4$ yr. The age derived under the assumption of $E_0 = 10^{51}$ ergs yields an age which brackets this value (see Table 1), while the age of the remnant under the assumption of a distance of 6 kpc is at least a factor of 2 too large. These data, therefore, indicate that G8.7−0.1 and PSR 1800−21 are coincident in age under the assumption of an initial SN explosion energy of 10^{51} ergs.

4.3. *The Morphology of G8.7−0.1*

The morphology of G8.7−0.1 at radio wavelengths is neither shell-like nor center filled (Frail et al. 1994b) with "plumes" observed notably in the south and along the western edge. In the 0.1–2.4 keV X-ray band (see Fig. 1*a*) an intensity discontinuity is observed with strong emission from around the northern half of the remnant (as defined by the radio). We investigated the possibility that the X-ray discontinuity was due to absorption effects (see § 3) by looking for hardness ratio variations anticorrelated with the intensity variations. No anticorrelation was found, implying that the discontinuity is not a result of absorption effects or gross spectral changes and another explanation must be sought. It is known, based on CO observations, that molecular gas is associated with W30 (Blitz et al. 1982). We therefore speculate that the supernova event which gave birth to PSR 1800−21 occurred in or near a molecular cloud at, or very near, the current position of the pulsar. In fact, Odegard (1986) first suggested, based on the morphology observed at 57.5 MHz, that the nonthermal component of W30 was emission from a SNR which occurred in a nonuniform medium and drew an anology between W30 and VRO 42.05.01 (G166.0+4.3), a SNR believed to have occurred within the bounds of a dense cloud and "blown out" into a "tunnel" in the ISM (Pineault, Landecker, & Routledge 1987). The properties of a supernova within or near a molecular cloud and the subsequent evolution of the remnant have been discussed by Tenorio-Tagle, Bodenheimer, & Yorke (1982, hereafter TBY). The simulations of TBY indicate that a supernova interacting with a molecular cloud (a) causes little or no disruption of the cloud, (b) leads to nonsymmetric remnant shapes due to the nonuniform medium into which the remnant is expanding, (c) causes a more rapid expansion into the less dense phase of the ISM than would be expected from expansion into an isotropic medium, and (d) can produce temperature gradients within the remnant. This scenario, a supernova in the vicinity of a molecular cloud complex, is very attractive when applied to the G8.7−0.1/PSR 1800−21 association in that it explains the peculiar radio morphology (the SNR is tracing out the least dense regions of the local ISM), explains the X-ray morphology (the intensity is largest in the northern extent due to a reflected shock from the molecular cloud complex sweeping through the supernova cavity and concentrating the hot X-ray emitting gas ahead of it), and removes the largest difficulty for the association in that a large transverse velocity is no longer required for PSR 1800−21 (the supernova occurred near the present position of the pulsar). In support of this scenario we note that the observed H II regions can be viewed as tracing out the boundaries of the molecular cloud complex and the inferred structure fits in well with our interpretation (see Kassim & Weiler 1990a, b). As a caveat, however, the model of an adiabatic remnant applied here may not be entirely applicable, and a detailed hydrodynamic simulation would be necessary to thoroughly address these observations. Such a simulation is presently unavailable and is beyond the scope of the present work.

We checked that the observed count rate of PSR 1800−21 was consistent with the assumption of a uniform column density across G8.7−0.1. To this end we modeled PSR

1800−21 as a twin of the Vela pulsar, owing to its dynamic similarity, and determined the necessary column density which yields the observed count rate of 1.5 ± 0.5 ks^{-1}. We adopted the spectral parameters of the Vela pulsar for both the compact point source and the compact nebula as given by Ögelman, Finley, & Zimmermann (1993). The results of the simulation indicate that the observed count rate is consistent with an absorbing column of $\leq 2 \times 10^{22}$ cm^{-2} for a distance of 6 kpc and $\leq 2.5 \times 10^{22}$ cm^{-2} for a distance of 4 kpc. Thus, the hypothesis of a uniform column density of 1.4×10^{22} cm^{-2} across G8.7−0.1 is consistent with the observed count rate of PSR 1800−21. Since previous radio observations reveal no compact nebula like that of Vela around PSR 1800−21, these limits are probably conservative.

5. SUMMARY

In summary, the X-ray data presented here support a G8.7−0.1/PSR 1800−21 association. The physical parameters of G8.7−0.1 are consistent with coincidence in space and age with PSR 1800−21 upon application of a Sedov-Taylor blast wave analysis for a SNR in the adiabatic phase of evolution with an initial energy of $E_0 = 10^{51}$ ergs. The peculiar morphology of G8.7−0.1 in both the radio and X-ray energy bands is speculated to arise from occurrence of the supernova event in the vicinity of a molecular cloud complex. This scenario has the additional benefit of not requiring a large transverse velocity for PSR 1800−21, evidence for which has not been observed (Frail et al. 1994), as the supernova event took place at or very near the present position of the pulsar. However, the disagreement of the magnitude of the kinematic radial velocities related to G8.7−0.1 ($\sim$38 km s^{-1}, Kassim & Weiler 1990a) and the H I absorption results for PSR 1800−21 (last absorption at $\sim$27 km s^{-1}; Frail et al. 1991) remains an outstanding problem for the association.

The authors would like to thank D. Frail, N. Kassim, and K. Weiler for the use of the radio map of W30 as well as for their comments on the text. We would also like to thank W. Sanders, R. Edgar, P. Plucinsky, M. Juda, and S. Snowden for assistance with the diffuse analysis and useful comments along the way. This project was supported in part by NASA grants NAG 5-2492 and NAGW-2643.

REFERENCES

Altenhoff, W. J., Downes, D., Pauls, T., & Schraml, J. 1978, A&AS, 35, 23
Blitz, L., Fich, M., & Stark, A. A. 1982, ApJS, 49, 183
Brand, A., & Blitz, L. 1993, A&A, 275, 67
Cioffi, D. F., McKee, C. F., & Bertschinger, E. 1988, ApJ, 334, 252
Clifton, T. R., & Lyne, A. G. 1986, MNRAS, 174, 267
Frail, D. A., Cordes, J. M., Hankins, T. H., & Weisberg, J. M. 1991, ApJ, 382, 168
Frail, D. A., & Kassim, N. E. 1994, private communication
Frail, D. A., Kassim, N. E., & Weiler, K. W. 1994b, AJ, 107, 1119
Hamilton, A. J. S., Sarazin, C. L., & Chevalier, R. A. 1983, ApJS, 51, 115
Handa, T., Sofue, Y., Naomasa, N., Hirabayashi, H., & Inoue, M. 1988, PASJ, 39, 709
Kassim, N. E., Hertz, P., Schuyler, D., & Weiler, K. W. 1994, ApJ, in press
Kassim, N. E., & Weiler, K. W. 1990a, ApJ, 360, 184
Kassim, N. E., & Weiler, K. W. 1990b, Nature, 343, 146
Odegard, N. 1986, 92, 1372
Ögelman, H., Finley, J. P., & Zimmermann, U. 1993, Nature, 361, 136
Pfeffermann, E., et al. 1986, Proc. SPIE, 733, 519
Pineault, S., Landecker, T. L., & Routledge, D. 1987, ApJ, 315, 580
Raymond, J. C., & Smith, B. W. 1977, ApJS, 35, 419
Reich, W., Furst, E., Steffen, P., Reif, K., & Haslam, C. G. T. 1984, A&AS, 58, 197
Snowden, S. L., McCammon, D., Burrows, D. N., & Mendenhall, J. A. 1994, ApJ, 424, 714
Taylor, J. H., & Cordes, J. M. 1993, AJ, 411, 674
Taylor, J. H., Manchester, R. N., & Lyne, A. G. 1993, ApJS, 88, 529
Tenorio-Tagle, G., Bodenheimer, P., & Yorke, H. W. 1985, A&A, 145, 70 (TBY)

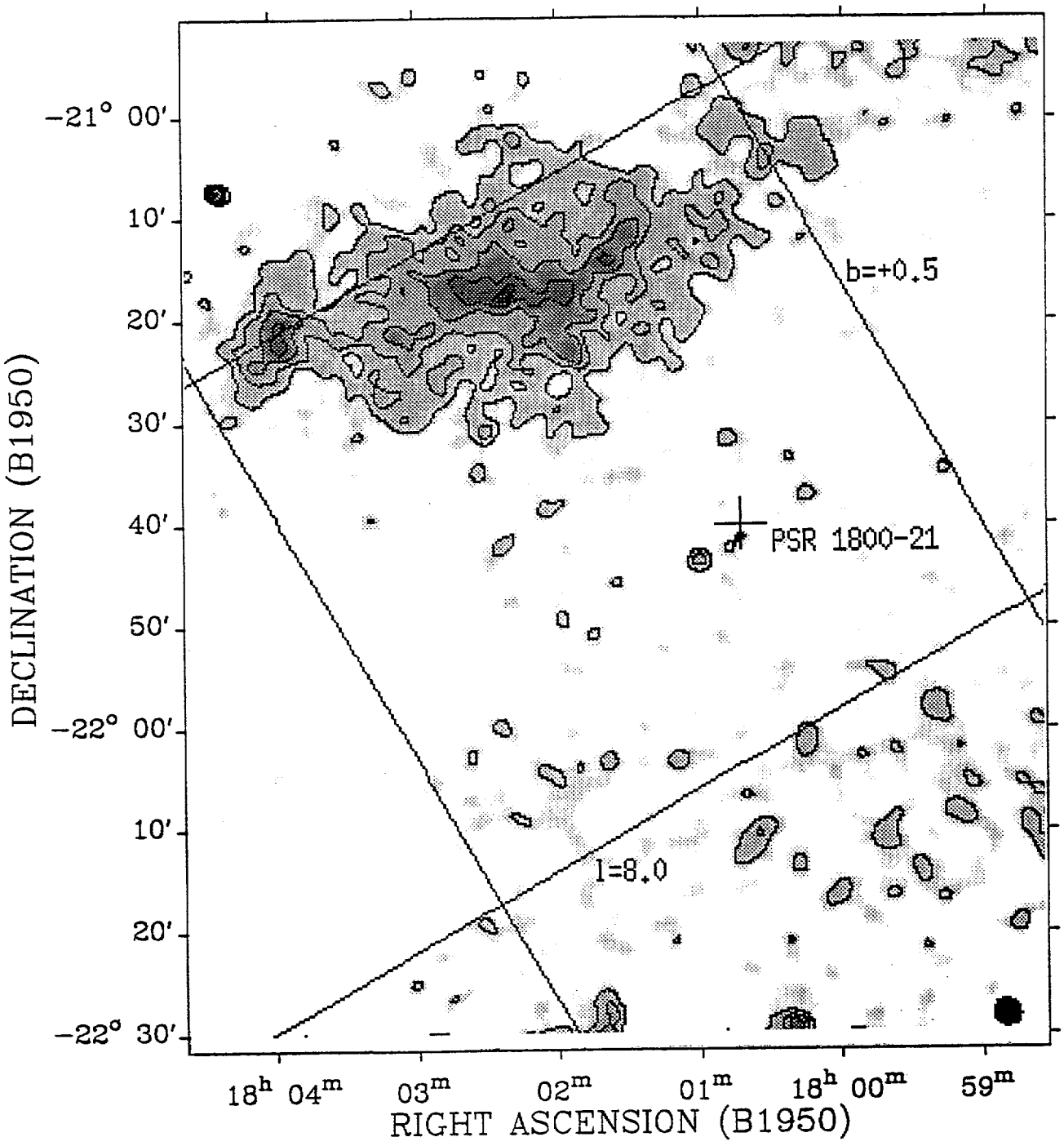

FIG. 1*a*

FIG. 1.—(*a*) Constant X-ray surface brightness contour map of the W30 complex in the 0.51–2.01 keV band. The map was vignetting corrected, dead time corrected, particle contamination corrected and flat-fielded using the energy-dependent exposure maps according to the prescription given by Snowden et al. (1994). prescription given by Snowden et al. (1994). The image was subsequently smoothed with a 2.5 FWHM Gaussian. The position of PSR 1800−21 is marked with a cross. Unrelated point sources were removed from the image. The contour levels are 0.8, 1.1, 1.4, 1.8, 2.1, 3.2, 6.4, 9.6, 12.8, and 16.0 counts ks^{-1} $arcmin^{-2}$. The lines mark $l_{II} = 8.0$, $l_{II} = 9.0$, $b_{II} = 0.5$ and $b_{II} = -0.5$ for ease of comparison with the radio map of Frail et al. (1994). The circular appearance of the image is due to the field of view of the *ROSAT* telescope. (*b*) Radio continuum image of G8.7−0.1 at 327 MHz from Frail et al. (1994b). The contour intervals are 10, 25, 50, 50, 75, 100, 150, 200, 300, and 400 mJy $beam^{-1}$. The position of PSR 1800−21 is indicated by the cross.